

Improved Driving Functions for Rectangular Loudspeaker Arrays

Driven by Sound Field Synthesis

Sascha Spors, Frank Schultz and Till Rettberg

Institute of Communications Engineering, University of Rostock, Richard-Wagner-Str. 31, 18119 Rostock, Germany

E-Mail: sascha.spors@uni-rostock.de

Introduction

Wave Field Synthesis (WFS) is a well-established sound field synthesis technique that uses a dense spatial distribution of loudspeakers (secondary sources) arranged around an extended listening area [1]. Practical systems are often of rectangular shape. It has been shown that the edges of such a loudspeaker array may result in considerable amplitude and spectral deviations in the synthesized sound field. This holds especially when using standard WFS driving functions [2].

In order to further investigate this effect, an analytic solution to the synthesis of a sound field by two semi-infinite secondary source distributions forming an edge is derived. This geometry serves as a prototype for the edges in rectangular setups. We use the equivalent scattering approach (ESA), that links the theory of sound field synthesis to acoustic scattering, for the derivation of the novel driving functions.

This paper is organized as follows: We briefly review the ESA in the next section, followed by the theory of scattering the field of a line source at an edge. This basis is then used to derive the novel driving functions which are finally evaluated by numerical simulations.

Equivalent Scattering Approach

We aim at synthesizing a sound field $S(\mathbf{x}, \omega)$ within a region V by a continuous distribution of monopoles (*single layer potential*) on the boundary ∂V . The synthesized sound field reads

$$P(\mathbf{x}, \omega) = \int_{\partial V} D(\mathbf{x}_0, \omega) G(\mathbf{x} - \mathbf{x}_0, \omega) dA(\mathbf{x}_0), \quad (1)$$

where $\mathbf{x}_0 \in \partial V$, $dA(\mathbf{x}_0)$ denotes a suitably chosen element for integration and $D(\mathbf{x}_0, \omega)$ the weight (driving function) of the secondary sources.

For ease of illustration we will first consider a two-dimensional (2D) scenario. For 2D synthesis, the free-field Green's function $G(\mathbf{x} - \mathbf{x}_0, \omega)$ is given by [3]

$$G_{2D}(\mathbf{x} - \mathbf{x}_0, \omega) = -\frac{j}{4} H_0^{(2)}\left(\frac{\omega}{c} |\mathbf{x} - \mathbf{x}_0|\right), \quad (2)$$

where $H_0^{(2)}(\cdot)$ denotes the Hankel function of second kind and zeroth-order, and \mathbf{x}_0 the position of the line source. We aim at the synthesis of the sound field of a line source $S(\mathbf{x}, \omega) = G_{2D}(\mathbf{x} - \mathbf{x}_s, \omega)$ where \mathbf{x}_s denotes its position.

Various approaches have been published to derive the driving function $D(\mathbf{x}_0, \omega)$ for the synthesis of a desired

sound field $S(\mathbf{x}, \omega)$. One of these is the equivalent scattering approach [4]. It states that the synthesis of a sound field by a single layer potential can be interpreted in terms of an equivalent acoustic scattering problem. The secondary source distribution acts as a notional object with homogeneous Dirichlet (i.e. sound-soft, pressure release) boundary conditions scattering the desired incident sound field $S(\mathbf{x}, \omega)$. Denoting the scattered field with $S_{sc}(\mathbf{x}, \omega)$, the total sound field reads

$$P_t(\mathbf{x}, \omega) = S(\mathbf{x}, \omega) + S_{sc}(\mathbf{x}, \omega). \quad (3)$$

The total sound field has to fulfill the Dirichlet boundary condition on ∂V

$$P_t(\mathbf{x}, \omega)|_{\mathbf{x}=\mathbf{x}_0} = 0. \quad (4)$$

The driving function for the ESA is given as the directional gradient of the total sound field [4, eq.(17)]

$$D(\mathbf{x}_0, \omega) = -\frac{\partial P_t(\mathbf{x}, \omega)}{\partial n(\mathbf{x}_0)}, \quad (5)$$

where

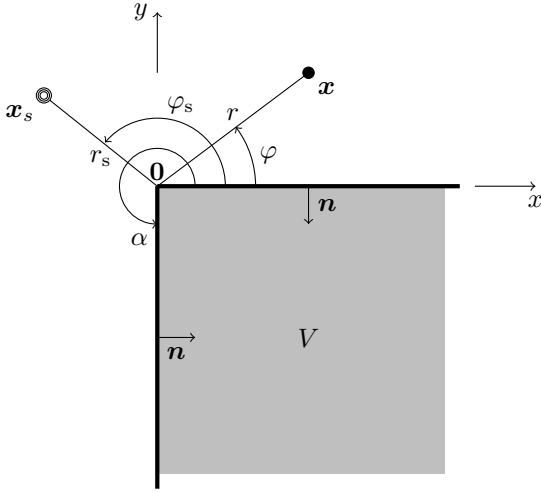
$$\frac{\partial P(\mathbf{x}, \omega)}{\partial n(\mathbf{x}_0)} = \langle \nabla_{\mathbf{x}} P(\mathbf{x}, \omega)|_{\mathbf{x}=\mathbf{x}_0}, \mathbf{n}(\mathbf{x}_0) \rangle \quad (6)$$

with $\langle \cdot, \cdot \rangle$ denoting the scalar product and $\mathbf{n}(\mathbf{x}_0)$ the inward pointing normal vector on ∂V at position \mathbf{x}_0 .

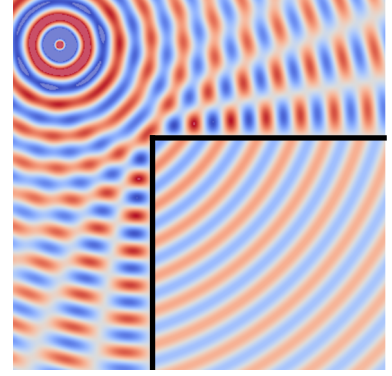
Scattering of a Line Source at an Edge

In order to apply the ESA, we need to consider the scattering of a line source at an edge with a Dirichlet boundary condition imposed. Solutions for this scattering problem under Neumann (sound-hard) or Dirichlet boundary conditions are presented in [5, 6, 7].

It is convenient to elaborate this scattering problem with the polar coordinate system. The geometry illustrated in Figure 1a is underlying the following considerations. The edge is located at the origin of the coordinate system. The outer angle of the edge is denoted by α . The position \mathbf{x} of a field point is given in polar coordinates by its angle φ and distance r from the origin. The same holds for the position of the source $\mathbf{x}_s \notin V$ with φ_s and r_s . Note that these angles have to be in the range $0 \dots 2\pi$. As outlined in [6], the solution [7, eq.(5.89) and (5.99)] for scattering at a sound-hard edge can be reformulated for sound-soft scattering. This results in the following



(a) Geometry



(b) Total sound field for $f = 500$ Hz, $r_s = 2.83$ m, $\varphi_s = 135^\circ$, $N = 400$

Figure 1: Sound-soft scattering of a line source at a two-dimensional edge for $\alpha = \frac{3}{2}\pi$.

modal expansion of the total sound field

$$P_t(\varphi, r, \omega) = -\frac{j\pi}{\alpha} \sum_{n=0}^{\infty} \frac{1}{\epsilon_n} \sin(\nu\varphi) \sin(\nu\varphi_s) \times \begin{cases} J_\nu(\frac{\omega}{c}r) H_\nu^{(2)}(\frac{\omega}{c}r_s) & \text{for } r \leq r_s \\ J_\nu(\frac{\omega}{c}r_s) H_\nu^{(2)}(\frac{\omega}{c}r) & \text{for } r > r_s \end{cases}, \quad (7)$$

where $\nu = \frac{n\pi}{\alpha}$ and $\epsilon_n = 1 + \delta[n]$. Above series has to be truncated for a practical implementation. In [7] a truncation to $N \approx \lceil 2\frac{\omega}{c}r\frac{\alpha}{\pi} \rceil$ elements is suggested. Figure 1b exemplarily shows the total sound field for the scattering of an incident line source at an edge with sound-soft boundaries.

Driving Function for a Virtual Line Source

As outlined above, the derivation of the driving function using the ESA requires to calculate the directional derivative of the total sound field. The geometry depicted in Figure 2 is underlying the following considerations. The position \mathbf{x}_0 on the secondary source distribution ∂V is denoted by φ_0 and r_0 . Evaluating the gradient of the total sound field in polar coordinates and considering that

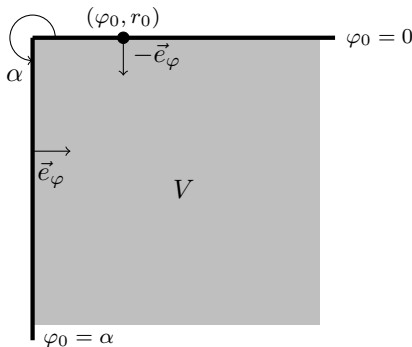


Figure 2: Geometry used for derivation of the driving function.

the normal vector onto the secondary source distribution has no component in the radial direction yields

$$D(\varphi_0, r_0, \omega) = -\frac{\partial P_t(\mathbf{x}, \omega)}{\partial n(\mathbf{x}_0)} = \pm \frac{1}{r} \frac{\partial P(\varphi, r, \omega)}{\partial \varphi} \Bigg|_{\substack{\varphi = \varphi_0 \\ r = r_0}} \quad (8)$$

for $\varphi_0 = \{0, \alpha\}$. The signs have to be chosen accordingly to the direction of the angular unit vector \vec{e}_φ in conjunction with the inward pointing normal vector \mathbf{n} of the secondary source distribution. The positive sign holds for $\varphi_0 = 0$ and the negative sign for $\varphi_0 = \alpha$.

The driving function is derived by introducing the total sound field (7) into (8) leading to

$$D(\varphi_0, r_0, \omega) = \mp \frac{j\pi}{\alpha} \sum_{n=0}^{\infty} \frac{1}{\epsilon_n} \cos(\nu\varphi_0) \sin(\nu\varphi_s) \frac{\nu}{r_0} \times \begin{cases} J_\nu(\frac{\omega}{c}r_0) H_\nu^{(2)}(\frac{\omega}{c}r_s) & \text{for } r_0 \leq r_s \\ J_\nu(\frac{\omega}{c}r_s) H_\nu^{(2)}(\frac{\omega}{c}r_0) & \text{for } r_0 > r_s \end{cases}, \quad (9)$$

for $\varphi_0 = \{0, \alpha\}$. The negative sign holds for $\varphi_0 = 0$, the positive sign for $\varphi_0 = \alpha$. Equation (9) constitutes the driving function for two-dimensional synthesis of a line source by a semi-infinite edge-shaped secondary source distribution. Its derivation required no approximations. However, the series has to be truncated for a practical implementation.

Driving Function for a Virtual Point Source using 2.5-Dimensional Synthesis

So far we considered the two-dimensional synthesis of a line source using secondary line sources. From a perceptual point of view, a line source is not desirable as virtual source due to its frequency response. The synthesis of a point source would be preferable. On the other hand, typical loudspeakers synthesize the field of a point source reasonable well. They do not synthesize the sound field of a line source.

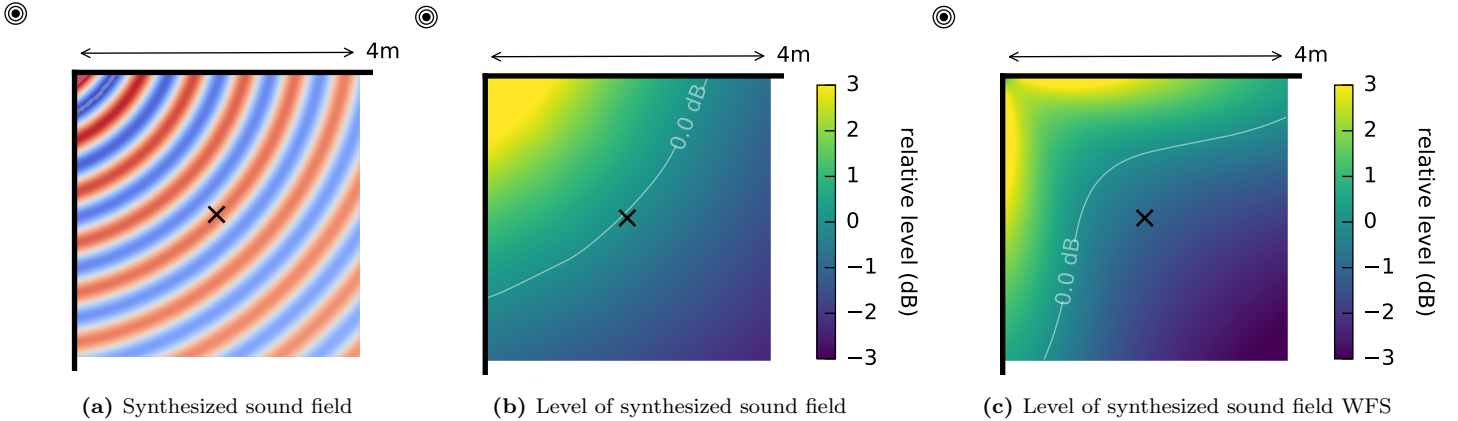


Figure 3: Two-dimensional synthesis of a monochromatic line source with a frequency of 500 Hz using the ESA. The line source is located at $r_s = 1.17$ m, $\varphi_s = 135^\circ$, the secondary source distribution is sampled with $\Delta x = 3$ mm, the total length of the distribution is 60 m. The real value of the complex pressure field $P(\mathbf{x}, \omega)$ is shown.

Let's assume the synthesis of a point source by monopole secondary sources located in a plane which is leveled with the listeners ears. This constitutes a 2.5-dimensional (2.5D) synthesis problem [8] due to the fact that it is essentially a two-dimensional problem but using secondary sources with the characteristics of the three-dimensional Green's function. In order to derive the driving function for this situation, the large argument approximation of the Hankel function [9]

$$-\frac{j}{4} H_0^{(2)}\left(\frac{\omega}{c} |\mathbf{x} - \mathbf{x}_0|\right) \approx \sqrt{\frac{1}{j \frac{\omega}{c}}} \cdot \sqrt{2\pi} |\mathbf{x} - \mathbf{x}_0| \cdot \frac{1}{4\pi} \frac{e^{-j \frac{\omega}{c} |\mathbf{x} - \mathbf{x}_0|}}{|\mathbf{x} - \mathbf{x}_0|} \quad (10)$$

is used, which holds for $\frac{\omega}{c} r \gg 1$. This approximation states that a line source can be approximated by a point source when applying filtering and an amplitude correction. The amplitude correction depends on the field point \mathbf{x} and consequently on the listener position. Hence, we have to consider a reference position \mathbf{x}_{ref} .

Assuming perfect synthesis of a line source, (10) can be introduced into the left- and right-hand side of (1). Isolating the point source contributions on both sides of the resulting equation, allows to derive the following corrected driving function for 2.5D synthesis

$$D_{2.5D}(\mathbf{x}_0, \omega) = \sqrt{\frac{|\mathbf{x}_{\text{ref}} - \mathbf{x}_0|}{|\mathbf{x}_{\text{ref}} - \mathbf{x}_s|}} \cdot D_{2D}(\mathbf{x}_0, \omega). \quad (11)$$

Results

Both the driving function for 2D, as well as for 2.5D synthesis of a line and point source are evaluated by numerical simulations. First the case of a continuous secondary source distribution is considered by simulating discrete secondary source distributions with a very high granularity. This way the effects of spatial sampling are assumed to be negligible.

Figure 3 illustrates the two-dimensional synthesis of a line source by an edge-shaped secondary source distribution using the driving function (9) with secondary line

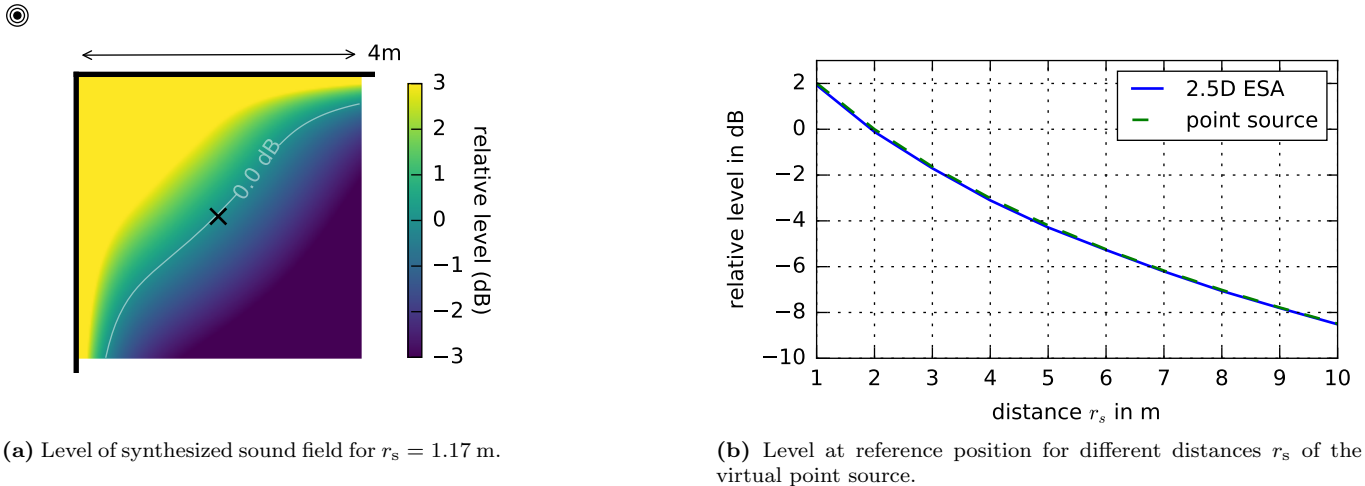
sources (2). The sound field is shown in Figure 3a indicating accurate synthesis. Figure 3b shows the absolute value (level in dB) of the synthesized sound field. The color scale has been normalized with respect to the level of the virtual line source at the indicated reference position (×). The level decay of a line source is accurately synthesized throughout the entire listening area. The result obtained for the same situation using a driving function for two-dimensional WFS is also shown for reference in Figure 3c (refer to [2] for more results using WFS).

Figure 4 illustrates the 2.5D synthesis of a point source by an edge-shaped secondary source distribution using the driving function (11) with secondary point sources. The theory of 2.5D synthesis outlined in the previous section predicts an amplitude mismatch for listener positions off the reference position. Figure 4a shows the level of the synthesized sound field. The color scale has been normalized with respect to the level of a virtual point source at the indicated reference position (×). A level mismatch, which decays with increasing distance to the secondary sources can be observed. This is a consequence of the secondary source type mismatch. The amplitude at the reference position for different distances r_s of the virtual point source is shown in Figure 4b. This result shows that the level of a point source is always reproduced correctly at the reference position.

The presented results have been derived by simulating a quasi-continuous secondary source distribution. In practice, the distance between the secondary sources has to be chosen larger. A detailed investigation of spatial sampling is out of the scope of this paper. However, preliminary results indicate that the loudspeaker density has to increase towards the edge.

Reproducible Research

All driving functions have been implemented in the Sound Field Synthesis Toolbox for Python, Version 0.3.1 [10]. The toolbox also includes driving functions for the synthesis of plane waves using the ESA. The code to reproduce the figures in this paper has been made



(a) Level of synthesized sound field for $r_s = 1.17$ m.

(b) Level at reference position for different distances r_s of the virtual point source.

Figure 4: 2.5-dimensional synthesis of a monochromatic point source with a frequency of 500 Hz using the ESA. The point source is located at $\varphi_s = 135^\circ$, the secondary source distribution is sampled with $\Delta x = 3$ mm, the total length of the distribution is 60 m. The real value of the complex pressure field $P(\mathbf{x}, \omega)$ is shown.

available as an electronic publication accompanying this paper [11].

Conclusions and Outlook

We have derived novel driving functions for the two-dimensional synthesis of a line source and the 2.5-dimensional synthesis of a point source with a semi-infinite edge-shaped secondary source distribution. For the former case it was shown that a perfect synthesis of the desired sound field is possible. Consequently, the artifacts which can be observed for WFS can be attributed to the assumption of a smooth secondary source distribution ∂V in its foundations. In the 2.5-dimensional case, unavoidable amplitude artifacts are present which can be accounted to the secondary source type mismatch. Following the same principles as outlined in this paper, driving functions for the synthesis of a plane wave have been derived. They show similar properties as the case of virtual line/point sources. The edge-shaped secondary source distribution serves as a prototype for the edges present in rectangular setups. Refer to [12] for an extension of the presented principles to a rectangular setup.

Acknowledgments

This work was conducted within the research group 'Simulation and Evaluation of Acoustical Environments (SEACEN)' supported by grant FOR 1557, Deutsche Forschungsgemeinschaft (DFG) and within the FET-OPEN project TWO!EARS supported by the EU FET grant ICT-618075.

References

- [1] A. Berkhout, "A holographic approach to acoustic control," *Journal of the Audio Engineering Society*, vol. 36, pp. 977–995, December 1988.
- [2] S. Spors, F. Schultz, and H. Wierstorf, "Non-smooth secondary source distributions in wave field synthesis," in *German Annual Conference on Acoustics (DAGA)*, March 2015.
- [3] E. Williams, *Fourier Acoustics: Sound Radiation and Nearfield Acoustical Holography*. Academic Press, 1999.
- [4] F. Fazi and P. Nelson, "Sound field reproduction as an equivalent acoustical scattering problem," *Journal of the Audio Engineering Society*, vol. 134, no. 5, pp. 3721–3729, November 2013.
- [5] A. Rawlins, "Plane-wave diffraction by a rational wedge," *Proceedings of the Royal Society of London. Series A, Mathematical and Physical*, vol. 411, no. 1841, pp. 265–283, June 1987.
- [6] M. Möser, *Technische Akustik*. Springer, 2012.
- [7] —, *Skript zur Vorlesung Theoretische Akustik*. Technische Universität Berlin, 2008.
- [8] S. Spors, R. Rabenstein, and J. Ahrens, "The theory of wave field synthesis revisited," in *124th Convention of the Audio Engineering Society*, May 2008.
- [9] "Digital library of mathematical functions," <http://dlmf.nist.gov/>.
- [10] S. Spors, M. Geier, and H. Wierstorf, "Sound field synthesis toolbox for python, version 0.3.1," 2016. [Online]. Available: <http://dx.doi.org/10.5281/zenodo.49356>
- [11] S. Spors, F. Schultz, and T. Rettberg, "Supplementary data in support of the paper: Improved driving functions for rectangular loudspeaker arrays driven by sound field synthesis," 2016. [Online]. Available: <http://dx.doi.org/10.5281/zenodo.49449>
- [12] F. Winter and S. Spors, "A comparison of sound field synthesis techniques for non-smooth secondary source distributions," in *German Annual Conference on Acoustics (DAGA)*, March 2016.